A hyperspectral view of the North Sea

Sindy Sterckx, Walter Debruyn

Vito, TAP, Boeretang 200, B-2400 Mol, Belgium
email: sindy.sterckx@vito.be

ABSTRACT

On the 16th of June 2003 a CASI hyperspectral airborne remote sensing campaign took place above the Southern North Sea, just offshore of Oostende. In coincidence with the airborne overpasses seaborne measurements of water leaving reflectance and water quality parameters were performed. In addition near-simultaneous satellite imagery are available. This paper describes the analysis of the airborne data. The CASI data have been atmospherically corrected using the software WATCOR which is based on the radiative transfer code MODTRAN and takes into account atmospheric and air/water interface effects. Two different approaches for atmospheric information retrieval were tested. In the first approach aerosol information and visibility are estimated from sun photometer measurements combined with MODTRAN radiative transfer simulations. The second method is based on an adapted dark-target approach to estimate the visibility. The results of both methodologies are comparable. The data are subsequently geometrically corrected with PARGE. A semi-analytical approach is used to retrieve the concentration of the water constituents: for chlorophyll determination a bio-optically modeled red/NIR band ratio algorithm is applied to the data; to quantify the Suspended Particulate Matter a single band NIR algorithm is used. The results of these semi-analytical methods were compared to an analytical approach where the water quality parameters are retrieved using a matrix inversion of the Gordon reflectance model.

Keywords: CASI, WATCOR, Chlorophyll, Suspended Matter, Coastal Waters, Hyperspectral

1 INTRODUCTION

On the 16th of June 2003 a BELCOLOUR airborne remote sensing campaign took place above the Southern North Sea, just offshore of Oostende. A Compact Airborne Spectrographic Imager (CASI) was installed in a Dornier 228 aircraft. The aircraft and CASI sensor was operated by NERC (Natural Environment Research Council), UK. The CASI was flown at an altitude of 2000 m, providing a spatial resolution of 4 m. The spectral configuration of the CASI was 96 channels from 405 to 947 nm with a FWHM of 6 nm. Eleven flight lines (line 13-23; lines are numbered according to the flight order) were flown in North-South or South-North direction. One flight line (line 24) was acquired in East-West direction for the study of bidirectional effects. The data were acquired between 11:57 and 13:39 GMT. The flight area covered two stations (130 and 230) where seaborne measurements were performed during the airborne data acquisition.

2 METHODS

2.1 Image pre-processing

The CASI data were delivered in spectral radiance units. Almost no information was provided on the quality of the radiometric and spectral calibration. To minimize the across-track illumination differences a normalization has to be performed. For this purpose an IDL code is written. First the average radiance value is calculated for each column of pixels (along track direction) of the CASI image (excluding the land pixels). A second degree polynomial function is then fitted to these column averages. By normalizing this polynomial function to the minimum value a correction factor for each column is calculated. Cross track illumination effects may be caused by vignetting effects, instrument scanning, direct sun reflection, or other non-uniform illumination effects [1].

Presented at the Airborne Imaging Spectroscopy Workshop, Bruges, 8 October 2004

2.2 Atmospheric and Air-interface Correction

2.2.1 WATCOR

The radiance received by the sensor L_{rs} consists of atmospheric path radiance $L_{atm-path}$, background path radiance $L_{rs,b}$ and ground reflected radiation L_{target} or

$$L_{rs} = L_{atm-path} + L_{rs,b} + L_{target} \tag{1}$$

with

$$L_{target} = \frac{d^*_{direct}(\tau,\theta_v) R_{app} E_d(a)}{\pi} \text{ and } L_{rs,b} = \frac{d^*_{diffuse}(\tau,\theta_v) A_{app} E_d(a)}{\pi}$$

where $E_d(a)$ is the downwelling irradiance above the water surface, $d^*_{diffuse}$ and d^*_{direct} are the diffuse and direct ground-to-sensor transmittance, R_{app} is the target apparent reflectance and A_{app} is the average or background apparent reflectance.

The air-water interface transfer can be written as:

$$R_{app} = \rho_{(a\to w)} + t_{(w\to a)} \frac{E_u(w)}{E_d(a)} = \rho_{(a\to w)} + t_{(w\to a)} R(0^-) t_{(a\to w)} \frac{1}{1 - s^*_{\text{int}} R(0^-)} \tag{2}$$

with $\rho_{(a\to w)} = \frac{\pi r(\theta_v) L_d(a)}{E_d(a)}$ the reflection function of the air-water interface, $L_d(a)$ the downwelling sky radiance above the water surface, $r(\theta_v)$ the Fresnel reflectance, $E_u(w)$ the upward irradiance just below the surface, $R(0^-)$ the subsurface irradiance reflectance, s^*_{int} the spherical albedo for illumination from below and $t_{(w\to a)}, t_{(a\to w)}$ the transmittance function of respectively water to air and air to water.

The atmospheric and air-interface correction is performed with the in-house software WATCOR. WATCOR uses the radiative transfer code MODTRAN-4 and follows the formulas given in Ref. 2. In a first step the at-sensor radiance is converted to apparent reflectance R_{app}. The apparent reflectance R_{app} can be estimated from the at-sensor radiance L_{rs} and the background radiance $L_{rs,b}$ (i.e. average radiance of surrounding pixels, calculated with a moving window technique) according to:

$$R_{app} = \frac{c_1 + c_2 L_{rs} + c_3 L_{rs,b}}{c_4 + c_5 L_{rs,b}} \tag{3}$$

where $c_1, \ldots, c_5$ are atmospheric correction parameters.

The formula to convert the apparent reflectance R_{app} to subsurface irradiance reflectance $R(0^-)$ is :

$$R(0^-) = \frac{-d_1 + R_{app}}{d_2 + s^*_{\text{int}} R_{app}} \tag{4}$$

where d_1 $(= \rho_{(a\to w)})$ and d_2 are the air-interface correction parameters.

2.2.2 Atmospheric characterisation

The CIMEL sun photometer (located in Oostende and integrated in the world-wide network AERONET) measured every 15 minutes the aerosol optical depth (AOD) at eight channels between 340 and 1020 nm. During the flight the AOD values varied around 0.76 at 340 nm, around 0.45 at 500 nm and around 0.10 at

1020 nm. The spectral dependence of the AOD can be described by the Angström exponent wavelength parameter α. Angström´s empirical relationship is given as:

$$AOD(\lambda) = \beta\lambda^{-\alpha} \tag{5}$$

During the flight campaign α varied around 1.65. Onboard of the Belgica research vessel the aerosol optical depth was also measured with a SIMBADA sun photometer. The Angström value extracted from the SIMBADA measurements at 443 - 670 nm varied around 1.6. The Angström exponent can be regarded as a spectral signature of the aerosol class. Higher values indicate a higher than average ratio of small particles to large particles [3]. A typical α value for the rural aerosol in MODTRAN-4 is 1.3 [4]. The α value for the maritime aerosol type is much smaller due to the relatively large salt particles. The α value for the standard urban aerosol in MODTRAN is also lower. Therefore from the standard MODTRAN aerosol types the rural aerosol seems to be the best guess.

The atmospheric correction result depends strongly on the visibility value used as input parameter. To estimate the visibility during the time the CASI data were acquired two different approaches were evaluated.

In the first methodology the visibility was estimated using MODTRAN-4 radiative transfer simulation combined with the sun photometer aerosol optical depth measurements. This procedure is similar to the approach given in [5] and is based on the fact that at 550 nm the aerosol optical depth is independent of the aerosol and atmospheric model and only varies with the visibility. For different input visibilities the aerosol transmittance was simulated with MODTRAN-4 and converted to aerosol optical depth values. These values were then compared to the sun photometer AOD measurements. Since there are no measurements at 550 nm the CIMEL AOD at 440 nm and 675 nm were interpolated to 550 nm using $\alpha_{440-675}$. For the SIMBADA the AOD at 550 was calculated using the AOD at 870 nm (no other channels were provided) and $\alpha_{443-670}$.

The second method is an adapted dark target approach and assumes that there is a pixel in the deeper water regions for which the water-leaving radiance is negligible in the near-infrared. Given equation 2 this implies that the apparent reflectance R_{app} equals the surface reflection $\rho_{(a\rightarrow w)}$. In this study the near-infrared band near 860 nm was used and the visibility is set by running WATCOR with a variety of reasonable visibility values until R_{app} equals $\rho_{(a\rightarrow w)}$ at 860 nm for the darkest pixel. This procedure was applied to each flight line (except the shorter line 23) using a rural aerosol.

The first approach resulted in an average visibility of (20.3 +/- 1.3) km. As given by the standard deviation the variation in the visibility during the flights was very small. The average visibility derived with the adapted dark target approach was (18.8 +/- 3.5) km. The variation in visibility, derived from this image-based approach, is however much higher (stdev = 3.5 km). Especially line 16 with a visibility of only 13 km can be seen as an outlier. Anyway the CIMEL data gave no evidence of a lower visibility at that moment. Based on these results it was decided to set the visibility to 20 km for the correction of all the flight lines. The results are in close agreement with the visibility (20 km) reported by the airport of Oostende.

2.3 Geometric Correction

For the geometric correction of the CASI lines the commercially available program PARGE (PARametric GEcoding) [6] is used. PARGE requires navigation, attitude and image/sensor information for the geocoding. The attitude (roll, pitch, heading) and position of the aircraft was measured during the flight with, respectively, an Inertial Measurement Unit (IMU) and a Global Positioning System (GPS). The aircraft GPS data are differentially corrected with a ground-based GPS of the FLEPOS (FLemish POsitioning Service) network. PARGE calculates first the 'theoretical viewing vector' using the aircrafts position (given by the dGPS) and scan angle. The 'theoretical viewing vector' is then transformed to the 'effective viewing vector' based on the attitude data. Because of the aircrafts motion some pixels in the final image contain no information from the scanner. These gaps are filled by a true nearest neighbor technique.

2.4 Water Quality Retrieval

In the first stage, a robust one-band algorithm [7] calibrated for the North Sea was used to derive the suspended matter content and for chlorophyll determination a well established Red/NIR ratio algorithm [8] was applied. The results of these semi-analytical methods were compared to an analytical approach where the water quality parameters are retrieved using a matrix inversion of the Gordon reflectance model.

2.4.1 The bio-optical modeling

Following Ref. 9 the relationship between the inherent optical properties (IOP) and the subsurface irradiance reflectance can be expressed as :

$$R(0-,\lambda) = f \cdot \frac{b_b(\lambda)}{a(\lambda)+b_b(\lambda)} \tag{6}$$

with $a(\lambda)$ the spectral total absorption coefficient (m^{-1}), $b_b(\lambda)$ the spectral total backscattering coefficient (m^{-1}) and f an empirical factor which depends on solar and viewing geometry and volume scattering in the water. In this paper f is set at 0.35 according to ref. 7.

The IOP $a(\lambda)$ and $b_b(\lambda)$ are linear functions of the constituents' concentrations. Equation (6) can therefore be written as (omitting the wavelengths) :

$$R(0-) = f \cdot \frac{b_{bw} + SPM \cdot b^*_{b,P}}{a_w + g440 \cdot \tilde{a}_{CDOM} + CHL \cdot a^*_{ph} + NAP \cdot a^*_{NAP} + b_{bw} + SPM \cdot b^*_{b,P}} \tag{7}$$

with

a_w	the absorption of pure water (m^{-1})
b_{bw}	the backscattering of seawater (m^{-1})
$g440$	CDOM absorption at 440 nm (m^{-1})
$\tilde{a}_{CDOM}$	CDOM absorption normalized by the absorption at 440 nm (m^{-1})
CHL	the concentration of chlorophyll-a (mg m^{-3})
NAP	the concentration of non-algal particles (g m^{-3})
SPM	the concentration of suspended matter (g m^{-3}) with $SPM = NAP + 0.07 \cdot CHL$ [10]
$b^*_{b,p}$	the specific backscattering coefficient of marine particles (m^2 g^{-1})
a^*_{ph}	the specific absorption coefficient of chlorophyll-a (m^2 mg^{-1})
a^*_{NAP}	the specific absorption coefficient of non-algal particles (m^2 g^{-1})

2.4.2 Chlorophyll retrieval : Gons algorithm

To derive CHL from the subsurface irradiance reflectance the Gons algorithm uses a ratio of two red bands: λ_1 located within a region of high chlorophyll-a absorption and λ_2 located within 700-740 nm. A near-infrared band λ_3 is used to estimate the backscattering. The following assumptions are used in the development of the Gons algorithm :

1. at λ_1 absorption other than Chl-a and water is negligible or $a(\lambda_1) = a_w + CHL \cdot a^*_{ph}(\lambda_1)$
2. at λ_2 a_{ph} , a_{CDOM} , a_{NAP} are insignificant in comparison with a_w or $a(\lambda_2) = a_w$
3. b_b is wavelength independent in the red/NIR region

In the study we used the CASI bands located at 671 nm (λ_1) , at 705 nm (λ_2) and at 774 nm (λ_3). Giving these 3 assumptions the Gons algorithm can be derived from equation (6) :

$$CHL = \frac{\left(\frac{R(0-,705) * (a_w(705) + b_b)}{R(0-,671)} - a_w(671) - b_b \right)}{a^*_{ph}(671)} \tag{8}$$

with

$$b_b = \frac{a_w(774) \cdot R(0-,774)}{f - R(0-,774)} \tag{9}$$

2.4.3 SPM retrieval

For the SPM retrieval a one-band algorithm calibrated for the Belgian coastal waters was used [7]:

$$MUMM - SPM = 111.21 \cdot \frac{\rho_w(708)}{0.187 - \rho_w(708)} + 4.46 \tag{10}$$

Since the coefficients in this algorithm have been calibrated for the MERIS sensor, the CASI ρ_w ($\rho_w = R_{app} - \rho_{(a \to w)}$ images were resampled to the MERIS bands in order to apply the algorithm. The MUMM-SPM product is defined to represent the suspended particulate matter concentration determined from measurements made on water samples taken from 3 m depth after filtration with a GF/C filter.

2.4.4 Matrix inversion

For m number of wavelengths equation (7) can be written as a linear system of equations :

$$y = A \cdot x$$

with

$$A_\lambda = \frac{R(0-,\lambda)}{f} \tilde{a}_{CDOM,\lambda} + \frac{R(0-,\lambda)}{f} a^*_{ph,\lambda} - b^*_{b,p,\lambda} 0.07 \left[1 - \frac{R(0-,\lambda)}{f} \right] + \frac{R(0-,\lambda)}{f} a^*_{NAP,\lambda} - b^*_{b,p,\lambda} \left[1 - \frac{R(0-,\lambda)}{f} \right]$$

and

$$y_\lambda = -a_{w,\lambda} \cdot \frac{R(0-,\lambda)}{f} + b_{b,w,\lambda} \left[1 - \frac{R(0-,\lambda)}{f} \right] \quad \text{with } \lambda = 1,..., m$$

and

$$x = \begin{bmatrix} CDOM \\ CHL \\ NAP \end{bmatrix} \tag{11}$$

To simultaneously estimate the concentrations of the water constituents a least-square approach was used for solving the system of linear equations. The inversion was performed using bands 8 to 53 (444 to 699 nm). Below 444 nm the CASI data were considered to be less accurate due to atmospheric/sky correction errors, relative insensitivity of the CASI sensor in this region and/or radiometric calibration problems at the shorter wavelengths [11]. Above 699 nm SIOPs data were not available for all the constituents.

The SIOPs used in the matrix inversion are based on in-situ measurements as well as literature values. a_w is taken from Ref. 12 and b_{bw} is given by Ref. 13. Following the methods of Ref. [14,15,16] the a^*_{ph}, a^*_{NAP} were determined from seawater samples taken from station 230 one day after the CASI flight. No backscattering measurements were performed in 2003 by the BELCOLOUR team. Therefore the average specific scattering coefficient determined by Ref. 17 from 56 samples of the North Sea was taken. This average value at 555 was 0.54 $m^2\ g^{-1}$ and the spectral dependence is given by $(\lambda/555)^{-0.4}$. A backscattering to total scattering ratio of 0.02 derived from the Petzold's volume scattering function was used to determine

the specific backscattering $b^*_{b,p}$ for the matrix inversion. An average $\tilde{a}_{CDOM}$ value derived from water samples taken at station 130 and 230 during cruises in April and May 2004 was used.

3 RESULTS

Figure 1 shows the result of the atmospheric correction. In the green, red and NIR parts of the spectrum a good correspondence between the airborne and in-situ reflectance spectra is obtained. Some differences in the absolute reflectance values can be due to the time difference between the in-situ measurements and the airborne data acquisition. Possible causes of the larger reflectance difference below 500 nm are inaccuracies in the sensor calibration or in the atmospheric aerosol characterization (standard MODTRAN-4 models used) and/or errors in the underlying model for the correction of the surface reflection effects at the air/water interface.

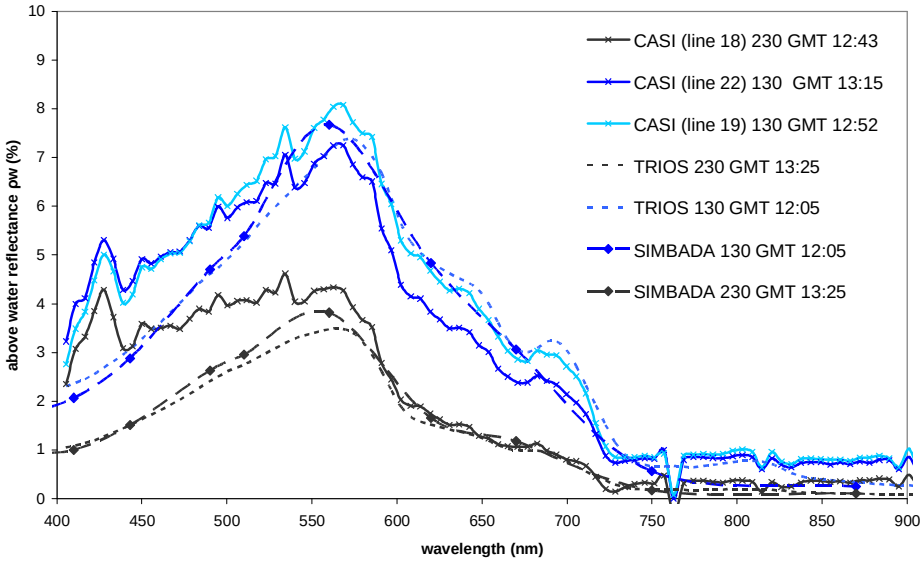

Figure 1. Comparison of ρ_w calculated from CASI images with ρ_w from in-situ measurements performed with TRIOS and SIMBADA spectrometers.

Water quality maps were calculated with the different algorithms (Fig. 2). Areas with negative values haven been flagged (black color). Adjacent flight lines are not acquired successively in time and time difference between the neighboring lines ranges from 15 minutes to almost one hour. This explains the shifts visible in the concentration of the water constituents between overlapping flight lines.

In the offshore area the chlorophyll-a concentrations derived with the Gons algorithm and with the matrix inversion algorithm are in good agreement. Closer to the coast the matrix inversion technique underestimates the chlorophyll-a concentration. Furthermore the obtained CDOM values (not showed) were often unrealistic (negative or low values). One possible cause can be an ill-chosen set of SIOP. The specific absorption coefficient of chlorophyll a^*_{ph} used in the matrix inversion was derived from the more offshore station 230 where the phytoplankton composition may be different from the near shore area; the b^*_p values were taken from the literature. Other possible causes may be inaccuracies in the atmospheric correction, insufficient information for retrieval of 3 independent parameters and the presumed CHL– SPM relationship.

The relative spatial distribution of the tripton concentration (NAP) derived with the matrix inversion technique and the SPM concentration from the MUMM-SPM algorithm are similar, but the absolute values differ strongly. The specific scattering value was taken from the literature and may not be accurate for the water composition at the time of recording. A second possible explanation for this is the difference in product terminology. The MUMM-SPM product represents the suspended matter concentration from

measurements made on water samples taken from 3 m depth after filtration with a GF/C filter while the NAP concentration derived from the matrix inversion technique is more representative of the surface layer.

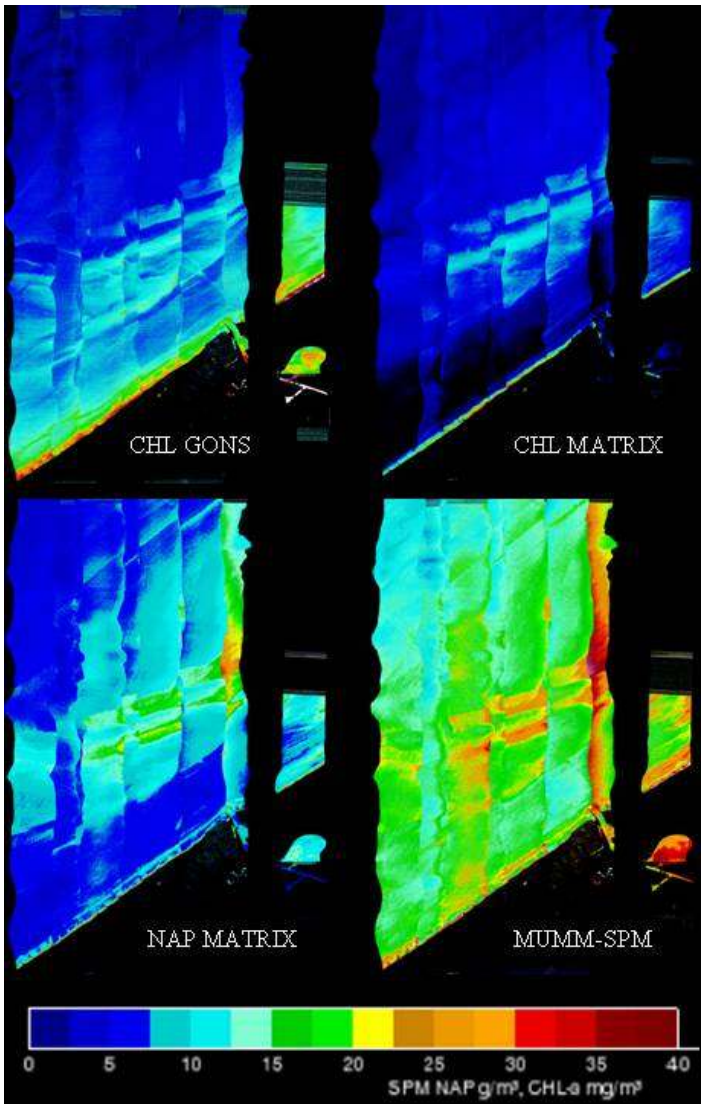

Figure 2. Maps of chlorophyll-a, suspended matter (SPM) and tripton (NAP) concentration derived with different water quality algorithms applied on hyperspectral airborne CASI data.

The algorithms were also applied to the in-situ reflectance measurements made at station 130 and 230 with the TRIOS spectrometer. The results are given in Table 1. The image derived concentrations for these two stations (average value for a 40 m x 40 m region around the stations) are also given. The concentrations of water quality algorithms applied to the in-situ reflectance spectra and the CASI spectra agreed very well, which may indicate that errors in chlorophyll and NAP retrieval caused by calibration and atmospheric correction inaccuracies are rather small. All algorithms resulted in concentrations which were significantly lower than the in-situ values. The chlorophyll concentration for station 130 and 230 retrieved with the matrix inversion technique was higher than obtained with the Gons algorithm. However based on visual inspection of the Chlorophyll maps (Fig. 2) we can see that this is not always the case for all pixels.

Table 1. Concentrations of the different water quality variables obtained from in-situ measurements (bold) and from the different water quality algorithms applied to both the CASI data and the TRIOS (italic) seaborne reflectance measurements.

STATION 130			STATION 230		
source	**GMT**	**concentrations**	**source**	**GMT**	**concentrations**
in-situ SPM (GF/F PA)[1] (g/m³)	**12:05**	**22.27**	**in-situ SPM (GF/F PA) (g/m³)**	**13:25**	**11.4**
in-situ SPM (GF/C)[2] (g/m³)	**12:05**	**36.40**	**in-situ SPM (GF/C) (g/m³)**	**13:25**	**13.33**
MUMM SPM (TRIOS) (g/m³)	*12:05*	*21.53*	*MUMM SPM (TRIOS) (g/m³)*	*13:25*	*8.18*
MUMM SPM (line 22) (g/m³)	13:15	16.26	MUMM SPM (line 18) (g/m³)	12:43	8.86
MUMM SPM (line 19) (g/m³)	12:52	19.97			
in-situ CHL a (GF/C) (mg/m³)	**12:05**	**16.60**	**in-situ CHL a (GF/C) (mg/m³)**	**13:25**	**3.64**
in-situ CHL a (GF/F) (mg/m³)	**12:05**	**13.76**	**in-situ CHL a (GF/F) (mg/m³)**	**13:25**	**8.57**
Gons Chl(TRIOS) (mg/m³)	*12:05*	*7.80*	*Gons Chl(TRIOS) (mg/m³)*	*13:25*	*0.74*
Gons Chl (line 22) (mg/m³)	13:15	4.85	Gons Chl (line 18) (g/m³)	12:43	2.01
Gons Chl (line 19) (mg/m³)	12:52	6.95			
Matrix Chl(TRIOS) (mg/m³)	*12:05*	*10.48*	*Matrix Chl(TRIOS) (mg/m³)*	*13:25*	*3.41*
Matrix Chl (line 22) (mg/m³)	13:15	6.35	Matrix Chl (line 18) (g/m³)	12:43	3.57
Matrix Chl (line 19) (mg/m³)	12:52	7.86			
in-situ NAP[3] (GF/F) (g/m³)	**12:05**	**21.31**	**in-situ NAP (GF/F) (g/m³)**	**13:25**	**10.80**
Matrix NAP (TRIOS) (g/m³)	*12:05*	*14.76*	*Matrix NAP(TRIOS) (g/m³)*	*13:25*	*3.08*
Matrix NAP (line 22) (g/m³)	13:15	9.99	Matrix NAP (line 18) (g/m³)	12:43	3.51
Matrix NAP (line 19) (g/m³)	12:52	13.77			

[1] Samples taken at 1 m depth on GF/F filters -PA: Pre Ashed

[2] Samples taken at 3 m depth on GF/C filters

[3] NAP = SPM (GF/F) - 0.07 CHL a (GF/F)

4 CONCLUSIONS

Different algorithms were applied to atmospherically corrected hyperspectral CASI data to produce maps of the concentrations of the water constituents. Since there are only two in-situ stations within the area it is difficult to assess the exact accuracy of water quality maps. Some difficulties were encountered with the matrix inversion technique. One of the goals at the end of the BELCOLOUR project is to produce a summary of SIOPs for the Belgian coastal waters. It is expected that significant improvements in the matrix inversion result will be achieved by using these more appropriate SIOPS. Furthermore, the use of a weighted least-square method [18] or using a smaller set of well-chosen bands (close to CHL and NAP features) [19] may improve the accuracy of the retrieved concentrations.

ACKNOWLEDGEMENTS

This study is part of the the BELCOLOUR project which is funded by the Belgian Science Policy Office's STEREO program. We thank the BELCOLOUR partners 'ULB and MUMM' for the in-situ and laboratory measurements; Jean Pierre DeBlauwe (MUMM) and their staff for establishing and maintaining the Oostende AERONET site used in this investigation and Luc Bertels (Vito) for assistance with the IDL programming.

REFERENCES

[1] RSI (2001). ENVI User's Guide. September 2001 edition. Research Systems.

[2] HAAN DE, J.F., KOKKE J.M.M.,1998: Remote sensing algorithm development toolkit 1. Operationalization of atmospheric correction methods for tidal and inland waters. Netherlands Remote Sensing Board (BCRS) publication. Rijkswaterstaat Survey Dept.

[3] DE LEEUW G., C. R. GONZALES, P. VEEFKIND, R. DECAE AND KUSMIERCZYK-MICHULEC, 2000: Retrieval of aerosol properties over land and over sea. ERS - ENVISAT Symposium, Gothenburg (S).

[4] GUEYMARD C., 1995: Simple model of the atmospheric radiative transfer of sunshine (SMARTS2): algorithms and performance assessment. FSEC-PF-270-95, Florida Solar Energy Center, Florida.

[5] KELLER, P., 2001: Imaging Spectroscopy of Lake Water Quality Parameters. PhD Thesis, Remote Sensing Series 36, RSL, University of Zurich.

[6] SCHLAEPFER D. AND RICHTER R., 2002: Geo-atmospheric Processing of Airborne Imaging Spectrometry Data Part 1: Parametric Orthorectification. *International Journal of Remote Sensing, 23(13)*,pp. 2609-2630.
[7] NECHAD B., DE CAUWER V., PARK Y., RUDDICK Y.,2003: Suspended Particulate Matter (SPM) mapping from MERIS imagery. Calibration of a regional algorithm for the Belgian coastal waters. European Space Agency. SP-549.
[8] GONS, H. J., 1999: Optical teledetection of Chlorophyll-a in Turbid Inlands Waters. *Environmental Science and Technology 33*, pp. 1127-1132.
[9] GORDON, H. R., BROWN, O. B., JACOBS, M.M., 1975: Computed relationship between the inherent and apparent optical properties of a flat homogeneous ocean. *Applied Optics 14(2)*, pp. 417-427.
[10] HOOGENBOOM, H.J., A.G. DEKKER, J.F. DE HAAN,1998: Retrieval of chlorophyll and suspended matter in inland waters from CASI data by matrix inversion. *Can. J. Remote Sensing 24(2)*, pp. 144-152
[11] JACOBSEN, A., K.B. HEIDEBRECHT, AND A.F.H. GOETZ, 2000: Assessing the Quality of the Radiometric and Spectral Calibration of CASI Data and the Retrieval of Surface Reflectance Factors, *PE & RS 66(9)*, pp. 1083-1091.
[12] H. BUITEVELD, J. M. H. HAKVOORT, M. DONZE, 1994: The optical properties of pure water. In: Jaffe , J. S. (ed): *SPIE Proceedings on Ocean Optics XII*,1994, 174-183.
[13] MOREL, A, 1974: Optical properties of pure sea water. In: G Jerlov and E N Steeman (ed.):Optical aspects of Oceanography. Academic Press, New York, pp. 1-24.
[14] TASSAN, S. AND G. FERRARI, 1995: An alternative approach to absorption measurements of aquatic particles retained on filters. *Limnol. Oceanogr.* 40(8),pp. 1358-1368.
[15] TASSAN, S. AND G. M. FERRARI, 2002:. A sensitivity analysis of the 'Transmittance-Reflectance' method for measuring light absorption by aquatic particles. *J. Plankton Res.* 24(8),pp. 757-774.
[16] FERRARI, G. AND S. TASSAN. 1999: A method using chemical oxidation to remove light absorption by phytoplankton pigments. *J. Phycol. 35*, pp. 1090-1098.
[17] BABIN, M., A. MOREL, V. FOURNIER-SICRE, F. FELL, AND D. STRAMSKI.,2003: Light scattering properties of marine particles in coastal and open ocean waters as related to the particle mass concentration. *Limnology and Oceanography 48*,pp. 843-859.
[18] HAKVOORT H., J. DE HAAN, R. JORDANS, R. VOS, S. PETERS AND M. RIJKEBOER, 2002 :Towards airborne remote sensing of water quality in The Netherlands - validation and error analysis. *ISPRS J. Photogramm. and Remote Sensing, 57*, 171-183.
[19] BRANDO VE, DEKKER, DA 2003: Satellite hyperspectral remote sensing for estimating estuarine and coastal water quality, *IEEE Transactions on Geoscience and Remote Sensing 41(6)*, pp. 1378-1387.